12-1-2002

Poly(Meta-phenylene Isophthalamide) Nanofibers: Coating and Post Processing

Wenxia Liu

Matthew Graham

Edward A. Evans
University of Akron Main Campus, evanse@uakron.edu

Darrell H. Reneker

Poly(meta-phenylene isophthalamide) nanofibers: Coating and post processing

Wenxia Liu
Maurice Morton Institute of Polymer Science, The University of Akron, Ohio 44325-3909
Matthew Graham and Edward A. Evans
Department of Chemical Engineering, The University of Akron, Ohio 44325-3909
Darrell H. Reneker
Maurice Morton Institute of Polymer Science, The University of Akron, Ohio 44325-3909

(Received 3 July 2002; accepted 26 September 2002)

Electrospun nanofibers have applications in the areas of filtration, composites, biomaterials, and electronics. Controlling the surface properties of these nanofibers is important for many applications. Nanofibers can also be used as unique substrates for observing the growth of deposited films and creating nanoscale structures. In this work, electrospun poly(meta-phenylene isophthalamide) (MPD-I) nanofibers were used as substrates for creating nanoscale structures out of carbon-based materials and metals. MPD-I was used because it can be electrospun into nanofibers with diameters smaller than 10 nm and it has good thermal stability. MPD-I nanofibers were coated with carbon, copper, and aluminum using plasma enhanced chemical vapor deposition and physical vapor deposition methods. Some of the aluminum-coated nanofibers were then converted into nanotubes. Transmission electron microscopy was used to determine the thickness, uniformity, and grain size of the coatings on the fibers and the nanotubes.

I. INTRODUCTION

Nanoscale materials have attracted great academic and industrial interest in recent years.[1–3] Electrospinning is a straightforward method for producing fibers with diameters in the nanometer range.[4–6] Since the 1990s, research efforts in electrospinning have focused on the mechanism of fiber formation,[4–10] the physical properties of nanofibers,[11–15] and the application of nanofibers in the areas of filtration,[16] composites,[17–20] biomedicine,[21–23] and electronics. High-performance nanofiber materials with improved and controlled surface properties are required for further development of these applications. Control over the surface of the nanofibers, achieved by coating the nanofibers, will lead to novel devices and structures. Recently, Greiner's group has shown that fibers can be coated by both sol-gel and thermally activated vapor deposition techniques.[24–25] Coating by chemical vapor deposition (CVD) or physical vapor deposition (PVD) offers an effective way to modify the surface properties of nanofibers. Subnanometer-thick coatings with high purity can be deposited by CVD and PVD techniques. Coatings with an average thickness smaller than 1 nm can be deposited. Bognizki *et al.,* for example, reported that electrospun poly(L-lactide) fibers could be coated with a variety of materials using thermally activated CVD and PVD techniques. These coated fibers were then used to form tubes by selectively removing the polymer fiber core.[26]

The synthesis of high-quality nanostructured ceramic materials by either CVD or PVD techniques normally requires high deposition temperatures (>200 °C). The nanofiber used as a substrate and/or template must be stable, therefore, above 200 °C. Poly(meta-phenylene isophthalamide) (MPD-I) has good thermal and mechanical stability. MPD-I fibers were commercialized by the Dupont company under the trade name of Nomex®. The thermal and mechanical stability and flame resistance of the fibers are attributed to the aramid groups and the three-dimensional hydrogen bond networks.[27,28] We reported previously on the electrospinning and characterization of MPD-I nanofibers.[14] MPD-I nanofibers were used in this work because they can withstand the higher deposition temperatures and can be selectively removed following coating by CVD or PVD. We coated MPD-I nanofibers with a variety of materials, including carbon, metals, and inorganic compounds, by plasma-enhanced CVD (PECVD) and plasma-enhanced PVD at temperatures in excess of 200 °C.

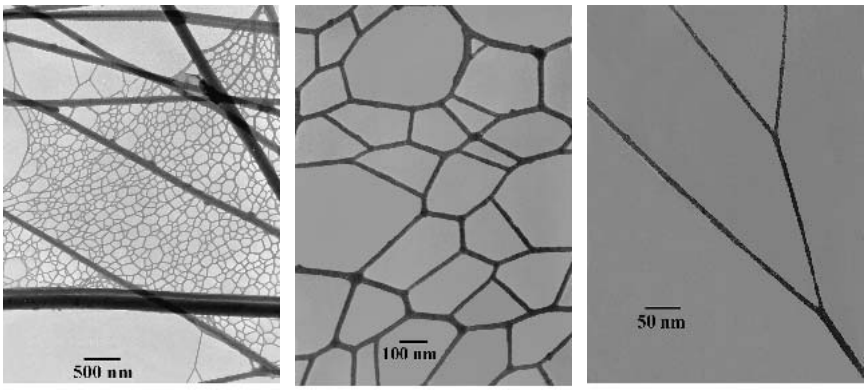

FIG. 1. (a,b) Weblike MPD-I nanofiber structure observed with a transmission electron microscope. (c) Branched MPD-I nanofibers with diameters less than 10 nm.

II. EXPERIMENTAL

The MPD-I nanofibers were produced using an electrospinning process. In a typical electrospinning process, a polymer solution is held in a pipette and a high voltage is applied between the solution and a conductive collector plate. A charged jet of the polymer solution is ejected when the forces of the applied electric field overcome the surface tension of the pendent drop at the tip of the pipette. The charged jet of polymer solution bends and elongates into spiraling loops. These loops grow larger in diameter as the jet travels and becomes thinner. As shown in previous papers,[4–6] the bending instability and other instabilities of the electrified polymer jet play central roles in the spinning process. After the solvent evaporates, nanofibers remain.

The MPD-I nanofibers were electrospun from a solution of 4% lithium chloride, 16% MPD-I, and 80% N-dimethylacetamide. The average molecular weight of the polymer was 90,000 g/mol. The spinning voltage was in the range of 15–25 kilovolts with a field strength of 10^5 volts per meter. The fibers were spun at room temperature.[14]

To load the fibers into the thin film deposition chamber, they were electrospun onto stainless steel washers or copper electron microscope grids. The fibers formed a nonwoven mat across the opening of the washers and grids. The washers and grids were placed on the sample holders.

The fibers were coated by plasma-enhanced CVD and PVD methods. Carbon films were deposited by PECVD and direct current (dc) magnetron sputtering. Hydrogenated amorphous carbon (a:CH) films were deposited on the surface of the nanofibers from a methane/argon mixture using an inductively coupled radio frequency (rf) plasma CVD system. The volumetric flow rates of methane and argon were 9 and 1 sccm, respectively. The deposition pressure was 35 millitorr. The fibers, which were supported on electron microscope grids, were placed directly on the cathode, which was water cooled, to maintain a temperature of less than 100 °C. The cathode was biased up to 500 V to generate the (a:CH) films. The deposition rate was on the order of 10 nm/min. The resulting films were continuous and translucent with a yellowish-brown color when collected on glass microscope slides. Carbon films were also deposited at 10 millitorr by dc magnetron sputtering. The rate of deposition was 8 nm/min. In the sputtering deposition, a titanium interlayer was used between the fiber and the carbon coating.

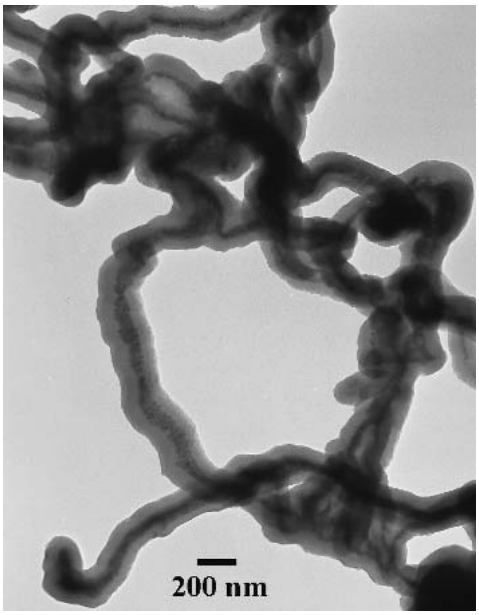

FIG. 2. TEM image of MPD-I fibers coated with carbon by CVD.

Copper and aluminum films were deposited onto the nanofibers by rf magnetron sputtering. The deposition was carried out at pressures between 10 and 50 millitorr

of argon. No bias was applied to the substrates. The substrate temperature was 150–200 °C for the sputtering processes. The substrate to target distance was 8 cm. The deposition rate varied between 3 and 24 nm/min, depending on pressure and power. Aluminum films were also deposited by thermal evaporation. The evaporation was carried out in argon, and the substrate temperature ranged from 180 to 200 °C. The distance between the evaporation source and the substrate was also 8 cm. The deposition rate during thermal evaporation was 2.4 nm/min.

III. RESULTS

MPD-I nanofibers were electrospun with diameters ranging from a few nanometers to around 200 nm. Figures 1(a) and 1(b) are transmission electron microscope (TEM) images showing weblike MPD-I nanofiber structures. These thin weblike structures, supported on other bigger MPD-I fibers, are frequently observed. Weblike fibers were also produced and observed by Bognitzki *et al.,* who referred to them as subnet fibers.[29] Figure 1(c) shows a TEM micrograph of a branched MPD-I nanofiber with diameter less than 10 nm. The thickness of the fibers is not uniform. The diameter of the thinnest section of the fiber at the upper right of the figure is only 4–5 nm. Possibilities for the formation of the branched fibers were discussed in Ref. 30; the fibers in Fig. 1 have much smaller diameters than those in Refs. 29 and 30.

Carbon films were deposited using both PECVD and dc magnetron sputtering. In both processes, the nanofiber substrates were exposed to carbon and argon ion bombardment from the plasma and were heated to temperatures greater than 100 °C. Figure 2 shows the carbon-coated fibers produced by PECVD. The MPD-I fibers are smaller than 100 nm in diameter. The thickness of the coating layer is in the same range as the fiber diameter. The interface of the carbon and the polymer can be distinguished due to the electron density contrast between the carbon and the polymer. The observation of a lower electron density of the carbon coating compared to MPD-I fiber can be explained by the presence of hydrogen in the carbon. At the conditions of deposition, a typical hydrogenated amorphous carbon has a hydrogen concentration of 40 atomic percent.[31] Also, the MPD-I fibers contained 17% lithium chloride, which was added to assist in the dissolution of the MPD-I[14] and remained in the nanofibers. The lithium chloride increased the observed electron density of the core of the fibers. Figure 3 shows TEM images of carbon films deposited by dc magnetron sputtering. The surface of the coating layer was rougher than the MPD-I fiber surface. Figure 3(a) is a high-magnification TEM image showing a 35-nm MPD-I fiber core coated with a 40-nm-thick carbon layer on the surface.

The MPD-I nanofibers were coated with copper and aluminum by the rf magnetron sputtering process (PVD). In the sputtering process the fibers were bombarded by argon and metal ions. The substrate temperature was kept below 200 °C. Figure 4(a) is a TEM image of copper-coated MPD-I nanofiber. The fiber is about 80 nm in diameter and the coating layer is about 20 nm thick. Strong electron diffraction rings from the copper layer were observed [Fig. 4(b)]. The d-spacings of the diffraction rings were 1.1, 1.3, 1.5, 2.1, 2.5 Å, which correspond to the reflections from the face centered cubic crystal unit cell of copper.[32] The surface of the copper coating layer was rough with peaks and valleys. The copper crystals had sharp edges. Small copper crystals, 10 nm in diameter, protruded in radial directions, although the diffraction pattern obtained from segments of the fiber showed no preferred orientation of the copper crystals. The

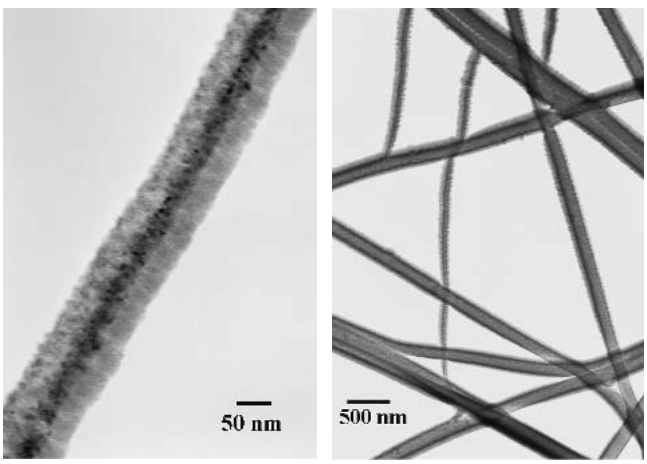

FIG. 3. TEM images of MPD-I fibers coated with carbon by dc magnetron sputtering.

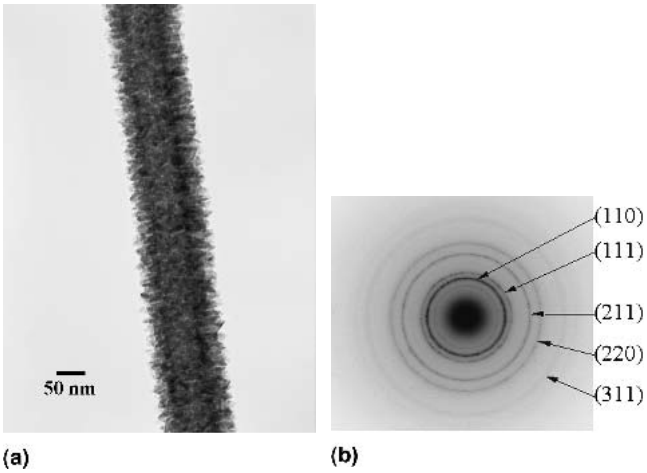

FIG. 4. (a) TEM image of a MPD-I fiber coated with copper by rf magnetron sputtering. (b) Electron diffraction pattern of copper coating in (a).

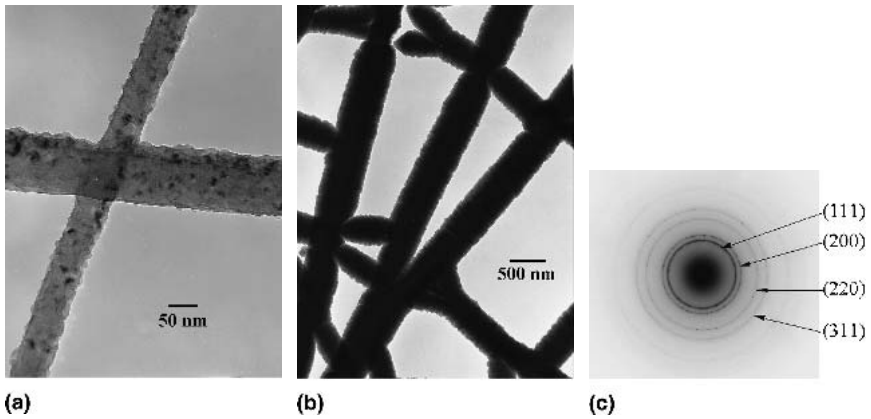

FIG. 5. (a,b) TEM images of MPD-I fibers coated with aluminum by rf magnetron sputtering. The thickness of the coated layers increases from about (a) 10 nm to (b) nearly 100 nm. (c) Electron diffraction pattern of the aluminum coating from (b).

density of sites on the polymer surface at which copper crystals nucleated and grew was more than 1 site per 100 nm.[2]

Figures 5(a) and 5(b) show aluminum-coated MPD-I fibers with different coating thicknesses. The coating on fibers in Fig. 5(b) is much thicker than that in Fig. 5(a). The sputtered aluminum formed small grains with diameters in the range of 15 to 30 nm, and heights of 10 to 20 nm [Fig. 5(a)]. These nanocrystalline films have about 10% of their mass in the surface layer or grain boundaries, which may significantly alter physical, chemical, and mechanical properties with respect to those of conventional coarse-grained polycrystalline materials.[33] Many properties of nanocrystal samples are found to be completely different from, and often superior to, those of conventional polycrystalline or amorphous solids.[34] The surface of aluminum metal is subject to oxidation in air. The most common oxide is amorphous oxide, which results from the exposure of aluminum metal to the atmosphere at room temperature. The oxide grows to a thickness of approximately 2 nm and then protects the underlying metal from further oxidation.[35] The d-spacings of the electron diffraction rings [Fig. 5(c)] of the coatings [in Fig. 5(b)] were 1.2, 1.4, 2.0, and 2.3 Å, which correspond to the (311), (220), (200), and (111) reflections from aluminum crystals, respectively, indicating that the dominant composition of the coating was still metal.[32] Figure 6 shows aluminum-coated weblike fibers. Most of the thin fibers in the web remained intact during the coating process, although some stubs of broken fibers are present. The surface of the aluminum-coated fibers was not as rough as that of the copper-coated fibers. The density of nucleation sites was about 1 site per 300 nm^2. In comparison to the carbon CVD coatings, the thicker PVD coatings are continuous but not uniform in thickness. The coatings are thicker where the fiber was exposed directly to the sputtering target. No appreciable structural difference was observed between the sputtered and evaporated aluminum films.

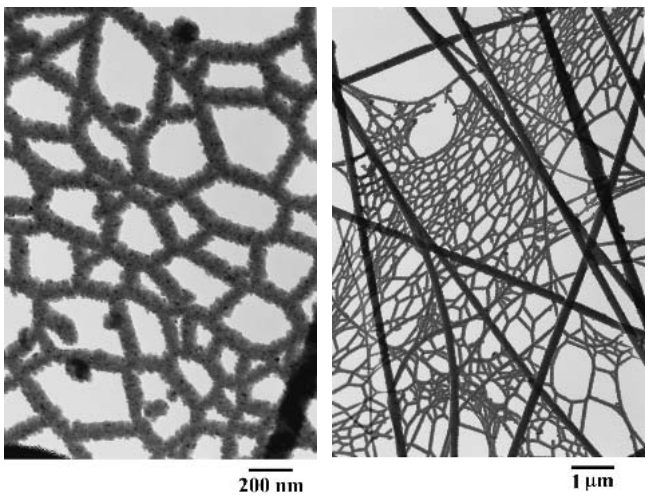

FIG. 6. The aluminum coated weblike fibers.

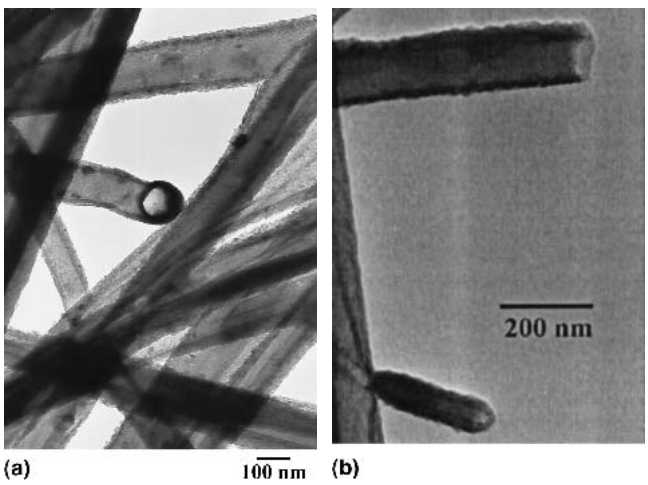

FIG. 7. (a) TEM image of Al_2O_3/Al nanotubes prepared by pyrolysis. (b) TEM image of two tube openings. The opening in the smaller tube is about 25 nm.

Polycrystalline aluminum nanotubes were created by heating the coated fibers at 600 °C for 10 min in air. The degradation of polymer is dependent on many factors,[36] one of which is temperature. Due to the rapid pyrolytic degradation of MPD-I above 370 °C,[37] the inner MPD-I fiber cores were removed. Tubular shells of the coating materials remained after the polymer was pyrolyzed. It is unclear whether all of the polymer was removed and if it was removed through the tube end or through the tube walls: this remains an important question. The tubes produced are similar to those reported by Bognitzki *et al.* but with smaller inner diameter.[26]

The outer diameters of the tubes were mostly in the range of 40 nm to 200 nm. The tube wall thickness was on the order of 10 nm. The cylindrical cross-section of a tube is shown in Fig. 7(a), which shows a tube segment that did not collapse after the polymer was removed. Ends of other such tubes are shown in Fig. 7(b). The smallest inner diameter observed was around 25 nm. The thickness of the wall of the tubes was controlled by the sputtering process. Tubes with different wall thicknesses are shown in Fig. 8.

Oxidation of aluminum is accelerated above 425 °C.[38–41] During the high-temperature annealing in air, part of the aluminum coating was oxidized. The electron diffraction pattern of the nanotubes [Fig. 8(c)] still shows reflections from (200) and (220) planes of aluminum crystals, but the (311) reflection almost disappeared, indicating the changing structure of the tube material. The diffraction ring with d-spacing of 2.4 Å may correspond to the (311) plane of face-centered-cubic Al_2O_3 crystals with a lattice of parameter 7.9 Å[39] rather than the (111) plane of Al crystals.

Aluminum tubes were also prepared by dissolution of the fiber cores by soaking the aluminum-coated MPD-I fibers in N,N-dimethylacetamide solvent for 6 h. After the MPD-I nanofibers were removed by solvent extraction, the aluminum tubes remained [Figs. 9(a)–9(c)].

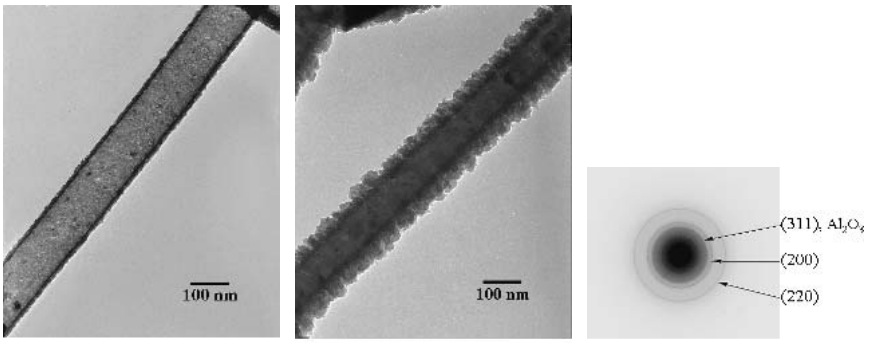

FIG. 8. (a) TEM image of an Al_2O_3/Al nanotube prepared by pyrolysis with tube wall thickness of about 10 nm. (b) TEM image of an Al_2O_3/Al nanotube with tube wall thickness of about 40 nm. The grain structure of the tube surface is shown. (c) Electron diffraction pattern of nanotubes prepared by pyrolysis.

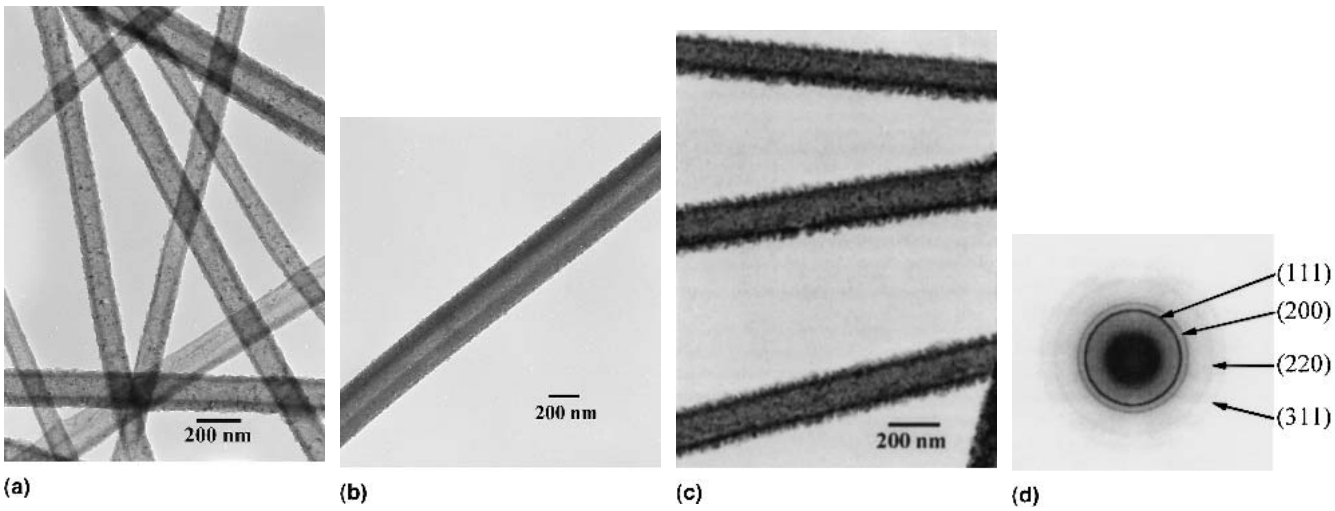

FIG. 9. (a–c) TEM images of Al tubes prepared by solvent dissolution of MPD-I fibers. (d) Electron diffraction pattern of nanotubes prepared by solvent dissolution of MPD-I fibers.

Figure 9(a) shows aluminum tubes with inner diameters of about 100 nm. Figure 9(b) shows an aluminum tube with a relatively smooth surface compared to tubes in Fig. 9(c). Solvent dissolution was used for preparation for other shapes of hollow shell structures shown in Refs. 42 and 43. Figure 9(d) shows the electron diffraction pattern of the aluminum tubes of Fig. 9(a). The d-spacings of the diffraction rings correspond to the aluminum crystal unit cell, which indicates that the aluminum layer did not oxidize during the dissolution process.

IV. SUMMARY AND CONCLUSIONS

MPD-I was used as a nanofiber material because it can be electrospun with diameters less than 10 nm and it is stable at high temperatures. The MPD-I nanofibers retain this stability even at the smallest diameters, as evidenced by the coating of the smallest fibers.

It has been shown previously that electrospun nanofibers can be coated using either a sol-gel technique or thermally activated processes.[15,26,42] In this work, we coated MPD-I nanofibers using plasma-enhanced deposition at elevated substrate temperatures. Coated nanofibers can be analyzed directly by TEM without additional thinning of the sample. Using TEM analysis, it has been shown that the plasma-coated nanofibers are coated in a single deposition step. As demonstrated by the formation of the nanotubes, the coatings are continuous around the nanofibers. The continuous coating results from the immersion of the fibers within the plasma. The fibers are supported across the opening of a washer or microscope grid. The boundary layer (sheath) between the plasma and the substrate is on the order of millimeters, several orders of magnitude larger than the fiber diameter. The ions and neutrals in the gas phase, therefore, can flow around and through the fiber mat to deposit material around the entire fiber; formation of the continuous coatings is proven by the subsequent formation of nanotubes. There is a limit to the thickness of the coating that can be achieved before the fibers break. We observed coatings as thick as 3 times the fiber diameter. These fiber samples can be used either as substrates for observation of the nucleation and growth process or creation of novel structures.

Nanotubes can be formed from the coated nanofibers by pyrolysis and/or dissolution; the process chosen affects the resulting tube properties. Nanotubes of mixed aluminum oxide and aluminum were produced by pyrolytic degradation of the MPD-I nanofiber cores. The aluminum coating layers underwent a limited degree of oxidation during pyrolysis of the MPD-I. The aluminum coating layers did not change when the template fiber was removed by dissolution. The average inner diameter of the tubes was around 100 nm. The smallest observed inner diameter of a tube was around 25 nm. The wall thickness of the tubes was in the range from 10 to 100 nm.

ACKNOWLEDGMENTS

This research was partially supported by the National Science Foundation in Grant Nos. CTS-9900949, "Nanofibers in Coalescence Filter Media" and DMI-9813098, "Manufacturing of Polymer Nanofibers by Electrospinning." Support also came from the Coalescence Research Consortium of the University of Akron.

REFERENCES

1. X. Duan, Y. Huang, J. Wang, and C.M. Lieber, Nature **409,** 66 (2001).
2. Y. Chi and C.M. Lieber, Science **291,** 851 (2001).
3. G. Stix, Scientific American **285,** 32 (2001).
4. D.H. Reneker, A.L. Yarin, H. Fong, and S. Koombhongse, J. Appl. Phys. **87,** 4531 (2000).
5. A.L. Yarin, S. Koombhongse, and D.H. Reneker, J. Appl. Phys. **89,** 3018 (2001).
6. H. Fong and D.H. Reneker, in *Structure Formation In Polymeric Fibers,* edited by D.R. Salem (Hanser, Cincinnati, OH, 2001), Chap. 6.
7. D.H. Reneker and I. Chun, Nanotechnology **7,** 216 (1996).
8. A.L. Yarin, S. Koombhongse, and D.H. Reneker, J. Appl. Phys. **90,** 4836 (2001).
9. Y.M. Shin, M.M. Hohman, M.P. Brenner, and G.C. Rutledge, J. Appl. Phys. Lett. **78,** 1149 (2001).
10. Y.M. Shin, M.M. Hohman, M.P. Brenner, and G.C. Rutledge, Polymer **42,** 9955 (2001).
11. H. Fong and D.H. Reneker, J. Polym. Sci.: Part B, Polym. Phys. **37,** 3488 (1999).
12. L. Huang, R.D. McMillan, R.P. Apkarian, B. Pourdeyhimi, V.P. Conticello, and E.L. Chaikof, Macromolecules **33,** 2989 (2000).
13. I.D. Norris, M.M. Shaker, F.K. Ko, and A.G. MacDiarmid, Synth. Met. **114,** 109 (2000).
14. W. Liu, Z. Wu, and D.H. Reneker, Polym. Prepr. (Am. Chem. Soc., Div. Polym. Chem.) **41,** 1193 (2000).
15. M. Bognitzki, W. Czado, T. Frese, A. Schaper, M. Hellwig, M. Steinhart, A. Greiner, and J.H. Wendorff, Adv. Mater. **13,** 70 (2001).
16. P.W. Gibson, H.L. Schreuder-Gibson, and D. Rivin, AlChE J. **45,** 190 (1999).
17. J.S. Kim and D.H. Reneker, Polym. Comp. **20,** 124 (1999).
18. J.S. Kim and D.H. Reneker, Polym. Eng. Sci. **39,** 849 (1999).
19. Y.A. Dzenis and D.H. Reneker, Proc. Am. Soc. Compos., Tech. Conf., 9th, 657 (1994).
20. M.M. Bergshoef and G.J. Vancso, Adv. Mater. **11,** 1362 (1999).
21. J.D. Stitzel, G.L. Bowlin, K. Mansfield, G.E. Wnek, and D.G. Simpson, Int. SAMPE Tech. Conf. **32,** 205 (2000).
22. D. Smith and D.H. Reneker, PCT Int. Appl. WO2001026702.
23. D. Smith, D.H. Reneker, W. Kataphinan, and S. Dabney, patent WO2001026610.
24. R.A. Caruso, J.H. Schattka, and A. Greiner. Adv. Mater. **13,** 1577 (2001).
25. H. Hou, Z. Jun. A. Reuning. A. Schaper, J.H. Wedorff, and A. Greiner, Macromolecules **35,** 2429 (2002).

26. M. Bognitzki, H. Hou, M. Ishaque, T. Frese, M. Hellwig, C. Schwarte, A. Schaper, J.H. Wendorff, and A. Greiner, Adv. Mater. **12,** 637 (2000).
27. H. Kakida, Y. Chatani, and H. Tadokoro, J. Polym. Sci.: Polym. Phys. **14,** 427 (1976).
28. H. Tadokoro, Jpn.-USSR Polym. Symp., 21 (1976).
29. M. Bognitzki, T. Frese, J.H. Wendorff, and A. Greiner, Preprints of the American Chemical Society Division of Polymeric Materials: Science and Engineering, **82,** 115 (2000).
30. S. Koombhongse, W. Liu, and D.H. Reneker, J. Polym. Sci.: Part B: Polym. Phys. **39,** 2598 (2001).
31. E.A. Evans, U. Hafeli, R. Wusirika, and P.W. Morrison, in *Amorphous and Nanostructured Carbon*, edited by J. Robertson, J.P. Sullivan, O. Zhou, T.B. Allen, and B.F. Call (Mater. Res. Soc. Symp. Proc. **593,** Warrendale, PA, 2000), p. 433.
32. B.D. Cullity, *Elements of X-Ray Diffraction*, 2nd ed. (Addison-Wesley, London, U.K., 1978).
33. L. Lu, Adv. Mater. **11,** 1127 (1999).
34. H. Gleiter, Prog. Mater. Sci. **33,** 323 (1989).
35. K. Wefers and C. Mistra, *Oxides and Hydroxides of Aluminum*, Alcoa Technical Paper No. 19 (Alcoa Laboratories, 1987).
36. M. Day, J.D. Cooney, K. Shaw, and J. Watts, J. Therm. Anal. **52,** 261 (1998).
37. A.A. Collyer, Mater. Sci. Technol. **6,** 981 (1990).
38. A.J. Brock and M.J. Pryor, Corros. Sci. **13,** 199 (1973).
39. K. Thomas and M.W. Robberts, J. Appl. Phys. **32,** 70 (1961).
40. P.E. Doherty and R.S. Davis, J. Appl. Phys. **34,** 619 (1963).
41. J.J. Randall and W.J.J. Bernard, J. Appl. Phys. **35,** 1317 (1964).
42. F. Caruso, X. Shi, R.A. Caruso, and A. Susha, Adv. Mater. **13,** 740 (2001).
43. Y. Lu, Y. Yin, and Y. Xia, Adv. Mater. **13,** 271 (2001).